ORIGINAL RESEARCH

Correlation of MR Relative Cerebral Blood Volume Measurements with Cellular Density and Proliferation in High-Grade Gliomas: An Image-Guided Biopsy Study

S.J. Price
H.A.L. Green
A.F. Dean
J. Joseph
P.J. Hutchinson
J.H. Gillard

BACKGROUND AND PURPOSE: As newer MR imaging techniques are used to assist with tumor grading, biopsy planning, and therapeutic response assessment, there is a need to relate the imaging characteristics to underlying pathologic processes. The aim of this study was to see how rCBV, a known marker of tumor vascularity, relates to cellular packing attenuation and cellular proliferation.

MATERIALS AND METHODS: Nine patients with histologically proved high-grade gliomas and 1 with a supratentorial PNET requiring an image-guided biopsy were recruited. Patients underwent a DSC study. The rCBV at the intended biopsy sites was determined by using a histogram measure to derive the mean, maximum, and 75th centile and 90th centile values. This measure was correlated with histologic markers of the MIB-1 labeling index (as a marker of glioma cell proliferation) and the total number of neoplastic cells in a high-power field (cellular packing attenuation).

RESULTS: There was a good correlation between rCBV and MIB-1 by using all the measures of rCBV. The mean rCBV provided the best results ($r = 0.66$, $P < .001$). The only correlation with cellular packing attenuation was with the 90% centile ($rCBV_{90\%}$, $r = 0.36$, $P = .03$). The increase in rCBV could be seen over 1 cm from the edge of enhancement in 4/10 cases, and at 2 cm in 1/10.

CONCLUSIONS: rCBV correlated with cellular proliferation in high-grade gliomas but not with cellular packing attenuation. The increase in rCBV extended beyond the contrast-enhancing region in 50% of our patients.

ABBREVIATIONS: CBV = cerebral blood volume; DSC = dynamic susceptibility-weighted contrast-enhanced perfusion MR imaging; max = maximum; MIB-1 = a monoclonal antibody directed against the Ki-67 antigen; NS = not significant; PET = positron-emission tomography; PNET = primitive neuroectodermal tumor; rCBV = relative CBV; $rCBV_{75\%}$ = 75th percentile CBV; $rCBV_{90\%}$ = 90th percentile rCBV; $rCBV_{max}$ = maximum rCBV; $rCBV_{mean}$ = mean rCBV; SPGR = spoiled gradient-recalled; VEGF = vascular endothelial growth factor; WHO = World Health Organization

The development of all tumors is dependent on having a sufficient blood supply. This is largely achieved by angiogenesis, a process that is carefully controlled by the local production of angiogenic growth factors. Studies that have quantified the extent of angiogenesis have shown that high-grade gliomas are the tumors most dependent on this process.[1]

During the past few years, MR imaging techniques have been devised that allow the noninvasive study of tumor vascularity. DSC, the most widespread technique in clinical practice, relies on the T2* signal-intensity change that occurs with the passage of a contrast agent through the tissues. This change allows calculation of the rCBV, a measure that has been shown to correlate with glioma vascularity[2,3] and the expression of VEGF.[4] These techniques may also tell us more about other pathologic changes that occur in tumors. Other studies have shown that tumors that have mitotic activity have a higher rCBV,[2,5] but these studies have included patients with both high- and low-grade tumors. This difference makes it difficult to determine whether the increase in mitotic activity directly relates to the tumor grade or the high rCBV.

There is an increasing interest in using these newer imaging methods as biomarkers to assist in tumor grading and biopsy guidance and to assess both progression and therapeutic response. It is, therefore, essential to understand their histologic basis. To further understand what the increase in rCBV tells us in a tumor, we have studied a more homogeneous group of high-grade gliomas undergoing image-guided brain biopsy. The aim was to assess whether rCBV values correlate with the tumor proliferation index (MIB-1 labeling index) and tumor cellular packing attenuation.

Materials and Methods

Patients

Patients with a solitary intracranial tumor (WHO grade III or IV) that required an image-guided biopsy were recruited for this study. The cohort for this study was part of a previously reported study that

Received June 4, 2010; accepted after revision July 23.

From the Academic Neurosurgery Division (S.J.P., P.J.H., J.H.G.) and Wolfson Brain Imaging Centre (S.J.P., H.A.L.G.), Department of Clinical Neurosciences; Department of Histopathology (A.F.D., J.J.), and University Department of Radiology (J.H.G.), University of Cambridge and Cambridge University Hospitals Foundation Trust, Cambridge, United Kingdom.

This work was funded, in part, by a grant from the New and Emerging Applications of Technology Program from the Department of Health, United Kingdom. P.J.H. is supported by the Academy of Medical Sciences/Health Foundation Senior Surgical Scientist Fellowship.

Please address correspondence to S.J. Price, MD, Academic Neurosurgery Unit, Box 167, Addenbrooke's Hospital, Hills Rd, Cambridge CB2 0QQ, UK; e-mail: sjp58@cam.ac.uk

DOI 10.3174/ajnr.A2312

correlated other MR imaging and PET parameters to histologic findings in a group of patients deemed likely to have high-grade gliomas on conventional imaging.[6,7] For this study, only patients with confirmed WHO grade III or IV tumors were included. All patients provided informed consent, and the study was approved by the local research ethics committee.

Imaging Studies

Patients were imaged approximately 48 hours before tumor biopsy by using a 3T MedSPEC S300 MR scanner (Bruker BioSpin, Ettlingen, Germany). All patients were imaged in the axial plane. The imaging protocol included a dual-echo T2/proton attenuation fast spin-echo sequence (TR, 6275 ms; TE, 120/20 ms; FOV, 16.8 × 35.8 cm^2; matrix, 256 × 512; 27 sections; acquisition time, 5 minutes 1 second) and a gradient-echo echo-planar imaging T2* DSC sequence (TR, 1500 ms; TE, 37.5 ms; FOV, 20 × 20 cm; matrix, 128 × 128; section thickness, 5 mm; 90 repetitions) with gadoteridol (ProHance; Bracco Diagnostics, Princeton, New Jersey) given as a bolus at a dose of 0.1 mmol/kg into a 20-ga cannula in the antecubital fossa by using a power injector at a rate of 3 mL/s initiated on the 10th repetition of the sequence (acquisition time, 2 minutes 20 seconds). An inversion-recovery T1-weighted sequence (TR, 3650 ms; TE, 45.2 ms; TI, 593.7 ms; FOV, 19.2 × 25.6 cm^2; matrix, 512 × 512; 19 sections; acquisition time, 5 minutes 30 seconds) and an SPGR 3D imaging (TR, 19.18 ms; TE, 5 ms; FOV, 25.6 × 25.6 × 25.6; matrix, 180 × 220 × 256 interpolated to 256 × 256 × 256 sections for reconstruction; 1-mm section thickness; acquisition time, 8 minutes 45 seconds) were performed after the administration of contrast.

Image-Guided Biopsy Procedure

All patients underwent a frameless image-guided biopsy. The contrast-enhanced 3D SPGR sequence was imported into a StealthStation Treon (Medtronic Navigation, Minneapolis, Minnesota) neuronavigation system. Image registration was performed by using Multitechnique Radiographic Scalp Markers (IZI Medical Products, Baltimore, Maryland) followed by a 40-point surface merge. When the residual error root mean square was >1.5, the image registration was repeated. The biopsy target was selected on the basis of contrast-enhanced T1-weighted images from the center of the tumor by an experienced neurosurgeon with help from an experienced neuroradiologist. Biopsies were performed with the use of a side-cutting 10 × 2 mm image-guided biopsy needle (Medtronic) and again were taken from the selected target and at 1-cm intervals back through the enhancing margin into apparently normal brain. Coordinates from each biopsy site were recorded and used for subsequent analysis. Postoperative imaging confirmed the accuracy of biopsies to be within 3 mm of the selected target by coregistering the postoperative 3D SPGR images (same parameters as above) by using vtkCSIG, Version 2.0.0 (Computational Imaging Sciences Group, Kings College, London, United Kingdom)[8] to the ones used for image guidance and by comparing the location of the actual biopsy tract with the biopsy coordinates.

Image Processing

Analysis of perfusion data was performed off-line by using a script written in Matlab (MathWorks, Natick, Massachusetts). Pseudo ΔR_2^* maps were created by using the following equation:

$$\Delta R_2^* = [\, -\ln(SI_t \,/\, SI_0) \,/\, TE].$$

The data were deconvoluted by using the method of Ostergaard et al,[9,10] and the arterial input function was created automatically by averaging the pseudo ΔR_2^* curves. CBV was then calculated by using the following equation:

$$CBV = \frac{k}{\rho}\left(\frac{\int R_t}{\delta R_2^* AIF}\right),$$

where ρ is a correction for the difference in attenuation between the brain and blood,[11] and k is a correction factor for the differences in hematocrit between the arteries and the capillaries such that

$$k = \frac{(1 - HCT_{arteries})}{(1 - HCT_{capillaries})}.$$

The perfusion images before the administration of contrast medium were coregistered to the SPGR sequence by using vtkCSIG,[8] and the nonrigid transformation matrix was used to coregister the rCBV maps to the SPGR images. Analysis of rCBV measures was performed by using ImageJ, Version 1.38x (developed by Wayne Rasband, National Institutes of Health, Bethesda, Maryland; http://rsb.info.nih.gov/ij/).

Determining Regions of Interest and Measures of rCBV

Regions of interest of 2 × 10 mm were placed by a researcher with 10 years of neuroimaging research experience and 12 years of neurosurgical planning for brain tumor biopsies on the SPGR image used for biopsy planning. The regions of interest were located in the regions where the biopsies were taken to allow the correlation of histologic features of the tumor with rCBV measurements. This was done by using the coordinates of the biopsy location obtained from the image-guidance system and placing the center of the region of interest at this location. The region of interest was oriented along the axis of the biopsy as determined from the image-guidance system. An example is show in Fig 1. The rCBV measures were made at each region of interest by using a histogram analysis method,[12] and values of $rCBV_{mean}$, $rCBV_{max}$, $rCBV_{75\%}$, and $rCBV_{90\%}$ were calculated for each region of interest. All rCBV measures were normalized to values taken from the contralateral white matter in the region of the centrum semiovale.

Histologic Processing and Analysis

At least 2 biopsies were obtained per location. A 0.5-mm section from the end of the biopsy core was removed for an intraoperative smear before the biopsies were fixed in 30% formyl saline for 1–3 days, processed for paraffin embedding, sectioned at 5-μm thicknesses, and stained with hematoxylin-eosin. Immunocytochemical staining was performed by using MIB-1. The Ki-67 antigen (DAKO, Glostrup, Denmark) is expressed when cells are in the cell cycle and not expressed in resting cells. Immunocytochemical staining was performed by using a 1/300 dilution, and MIB-1 sections were pretreated by microwave at high power in a buffer for 3 minutes. Negative controls omitted the primary antiserum, and sections of human tonsils were used as positive controls. Visualization was achieved by using an avidin-biotin-complex kit (ABC; DAKO) and diaminobenzidine as a chromogen. Biopsy specimens were examined by an experienced neuropathologist who was blinded to imaging findings. Tumors were graded according to WHO 2007 criteria by using all the biopsy material, as is standard pathologic practice. The MIB-1 labeling index was estimated for each biopsy site from the MIB-1-stained sections. Two adjacent high-power (×40 objective) digital photomicrographs were taken of the qualitatively assessed region of highest cellular packing

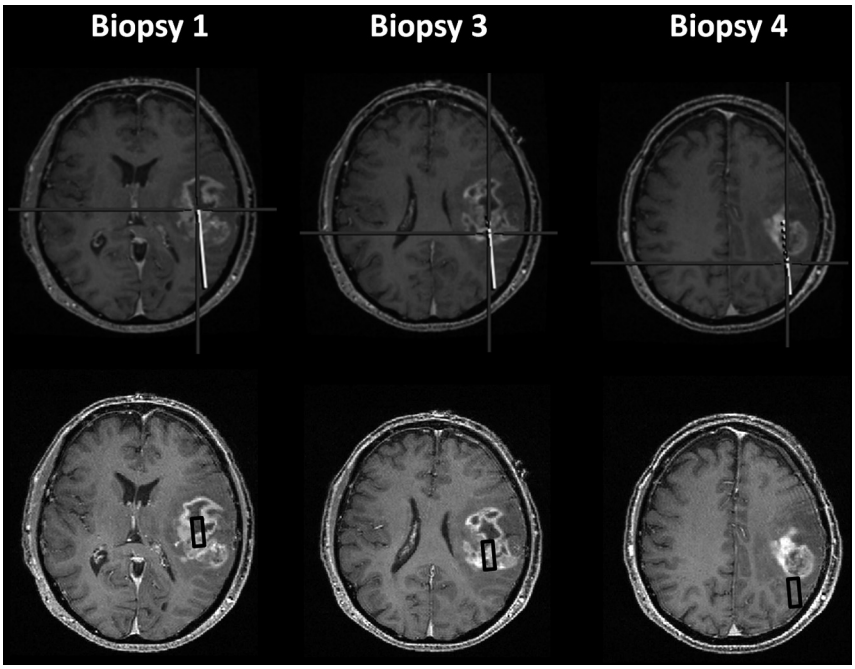

Fig 1. An example of how the regions of interest were determined in this patient with a glioblastoma. The upper panel shows the images from the image-guidance system, and the lower panel shows the SPGR image with the region of interest corresponding to this biopsy site (*black box*). The center of the region of interest is located at the biopsy site, and the orientation is in line with the biopsy tract.

attenuation. The number of nuclei (excluding endothelium and obvious inflammatory cells) were counted and recorded as tumor cellular packing attenuation. The MIB-1 labeling index was expressed as the percentage of positive nuclei.

Statistical Analysis

Statistical analysis was performed by using the Statistical Package for the Social Sciences for Windows (release 14.0.0, 2005; SPSS, Chicago, Illinois). Measures of cellular packing attenuation, the MIB-1 labeling index (the proliferation rate), and measures of rCBV were assessed for normality by using a single-sample Kolmogorov-Smirnov test. Correlations between rCBV measures and cellular packing attenuation and proliferation rates were performed by using the Pearson coefficient. Significance was assessed at the $P < .05$ level.

Results

Patients

In total, 21 patients were recruited to this study. In 9 patients, the overall diagnosis was not a high-grade tumor (8 low-grade gliomas, 1 cerebral lymphoma), and in a further 2 patients with glioblastomas, there was a technical failure in perfusion imaging that meant that the data could not be used. Overall 10 patients (8 men; mean age, 57 years; range, 23–79 years) with a confirmed high-grade tumor were recruited for this study. Table 1 summarizes the data on these patients. In all 10 patients, the image-guided biopsy was performed successfully without complications. The histology of the tumor revealed 1 WHO grade III tumor—an anaplastic oligoastrocytoma—and 9 WHO grade IV tumors (6 glioblastomas, 2 glioblastomas with an oligodendroglial component, and 1 supratentorial primitive neuroectodermal tumor). In total, 38 biopsies were obtained (range, 2–6; median, 4). The biopsy tract went into normal brain in 4 cases and into the infiltrating margin in 3 cases. In the remaining 3 cases, biopsies were only obtained from the tumor. Biopsies were taken from enhancing areas on T1-weighted imaging in 32 regions of interest and from outside the region of enhancement in 6 regions of interest.

Table 1: Patient details

No.	Age/ Sex	WHO Grade	Histology
1	42 M	III	Anaplastic astrocytoma
2	75 M	IV	Glioblastoma
3	60 M	IV	Glioblastoma
4	55 F	IV	Glioblastoma
5	32 M	IV	Glioblastoma
6	72 M	IV	Glioblastoma
7	79 M	IV	Glioblastoma
8	67 M	IV	Glioblastoma with oligodendroglial component
9	66 F	IV	Glioblastoma with oligodendroglial component
10	23 M	IV	PNET

Table 2: Correlation coefficients for different rCBV measures and MIB-1 index

rCBV Measure	Correlation Coefficient	*P* Value
$rCBV_{mean}$	0.66	<.001
$rCBV_{max}$	0.56	<.001
$rCBV_{75\%}$	0.60	<.001
$rCBV_{90\%}$	0.58	<.001

Correlation of rCBV and Histologic Features

There was good correlation between all the measures of rCBV and the MIB-1 labeling index (Table 2). The mean rCBV provided the best correlation with the highest *r* value ($r = 0.66$, $P < .001$) (Fig 2), and the maximum rCBV provided the lowest *r* value ($r = 0.56$, $P < .001$). There was poor correlation between measures of rCBV and cellular packing attenuation

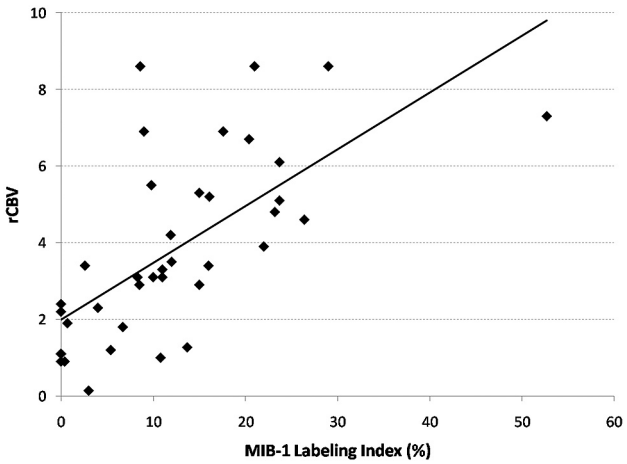

Fig 2. Graph shows the correlation between mean rCBV values and the MIB-1 labeling index. There is a good correlation between these parameters—a finding that was mirrored by the other measures of rCBV.

Table 3: Correlation coefficients for different rCBV measures and cellular packing density

rCBV Measure	Correlation Coefficient	*P* Value
$rCBV_{mean}$	0.09	NS
$rCBV_{max}$	0.29	NS
$rCBV_{75\%}$	0.19	NS
$rCBV_{90\%}$	0.36	.03

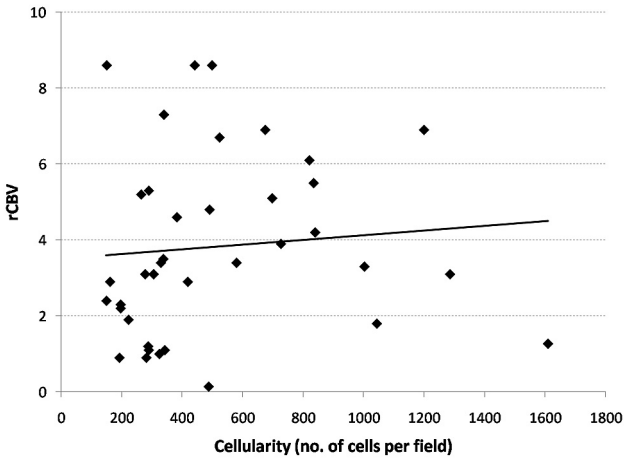

Fig 3. Graph shows a lack of correlation between rCBV and cellular packing attenuation. The results shown here for mean rCBV are mirrored by the other measures of rCBV, except the $rCBV_{90\%}$, which showed a correlation.

(Table 3 and Fig 3). Only $rCBV_{90\%}$ showed a weakly significant correlation ($r = 0.36$, $P = .03$). Even when the regions of interest obtained just from tumor were analyzed, there was still no correlation. Similar findings were also seen from regions of interest both within and outside the region of contrast enhancement.

In the 6 patients in whom the biopsies went outside the region of contrast enhancement, in 4, the mean rCBV value was >1.2 (a value previously suggested as a threshold that can differentiate tumor from normal brain[13]). In 3, this increased rCBV extended 1 cm from the enhancing tissue; in 1 patient, it extended 2 cm from the edge of the enhancement. An example is shown in Fig 4. In all patients, the histology of these areas corresponded to regions of tumor invasion of normal brain.

Discussion

The development and maintenance of an adequate blood supply are essential for tumor growth and invasion. Once tumors grow beyond a few millimeters, they cannot obtain sufficient oxygen and nutrients from diffusion alone. Experiments performed 70 years ago showed that if small tumors are implanted into the avascular region of the anterior chamber of the eye, they survive but do not grow beyond 2–3 mm.[14] These tumors can be removed after a year and implanted into a vascular tissue where they develop a blood supply and grow rapidly. The development of this new vasculature is controlled by secreted angiogenic factors such as VEGF or interleukin-8. Secretion of these factors is commonly controlled by hypoxic stimuli—VEGF production is controlled by hypoxia-inducible factor 1, which upregulates VEGF in the presence of hypoxic conditions. The number of cells in a region of tumor as well as the proliferation rate may influence this hypoxia-driven angiogenesis. This study aimed to see if proliferation or cellular packing attenuation was a determinant of tumor vascularity as measured by perfusion MR imaging.

By comparing histologic changes on image-guided biopsies with image-based measures of perfusion, we have shown that rCBV correlates with tumor proliferation (measured by the MIB-1 labeling index) and not with tumor cellular packing attenuation. This correlation would suggest that increased tumor vascularity, a well-recognized histologic correlate of rCBV,[2,3] is more dependent on cellular proliferation than just the number of cells present. Presumably, this is due to the drive of cellular proliferation and angiogenesis caused by tumor hypoxia. Although other studies have suggested that proliferation may correlate with rCBV, those studies have measured proliferation as the presence or absence of mitotic figures.[2,5] Similarly, the relationship of rCBV to cellular packing attenuation was assessed by using qualitative scales of minimal, intermediate, or attenuated cellular packing.[2] Sadeghi et al found that the cell attenuation only correlated with rCBV when the pure tumor samples were included,[15] a finding we could not replicate.

More recent studies characterizing tumor perfusion by using arterial spin-labeling in a variety of brain tumors showed that there was good correlation between semiquantitative measures of perfusion and both tumor vascularity and the MIB-1 index.[16] Arterial spin-labeling is an attractive method of assessing tumor perfusion because it can be quantified, is repeatable, and does not have the problems associated with contrast agents. This is, however, a method that is still in development and not yet in widespread routine clinical use and is unlike the contrast-flow methods that were used in our study.

This study has also shown that the rCBV abnormality extended beyond the area of tumor enhancement in 4 of the 6 cases in which biopsies were taken outside the area of contrast enhancement. This increased rCBV could be found ≤2 cm from the edge of enhancing tumor. Other studies have shown increased rCBV extending beyond the enhancing margin but have not been able to correlate these findings with the histology of invasive tumor.[13,17,18] This increase in rCBV probably

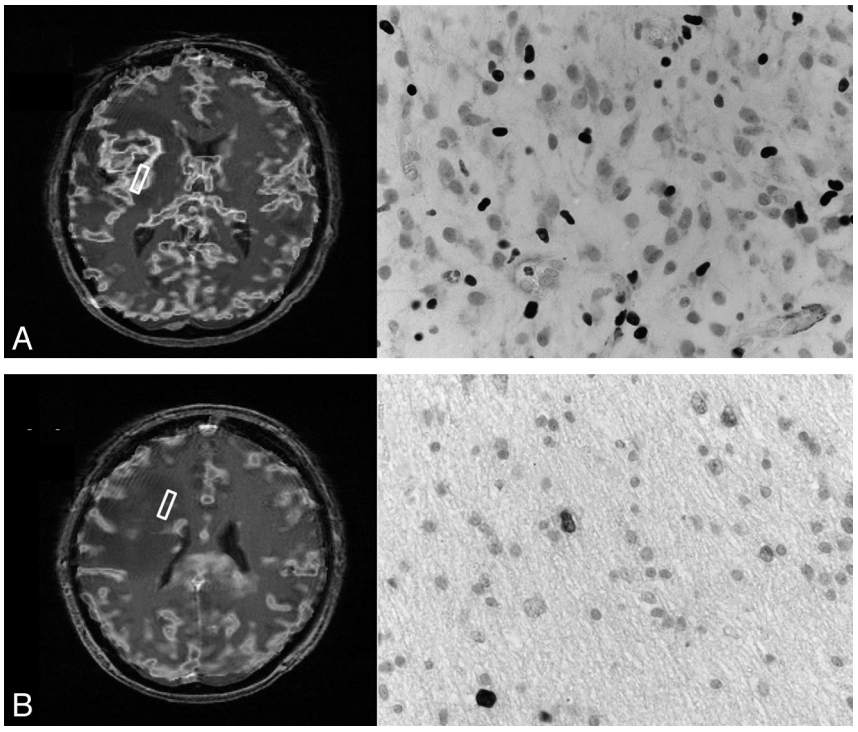

Fig 4. An example of the perfusion imaging and photomicrographs of MIB-1 immunohistochemistry (×40) from 2 biopsy sites in a patient with a glioblastoma. *A,* A biopsy obtained at the center of the tumor. The rCBV mean is 8.1 and the MIB-1 labeling index is 33%. *B,* A second biopsy site was obtained 2 cm from the edge of the contrast-enhanced region. The mean rCBV is elevated at 2.3, and histology showed that the MIB-1 was 3.5% in this sparsely cellular region.

relates to the increase in angiogenesis occurring in the infiltrating margin. Studies in pediatric brain tumors[19] and meningiomas,[18] however, have failed to show this extension of increased rCBV beyond the T1-weighted contrast-enhanced abnormality, a difference that probably relates to the less invasive pathology of these tumors.

Although selection of the regions of interest was determined by the location of the biopsy, the choice of the measure of rCBV was less clear. The mean rCBV for the region of interest may provide a misleading measure because it compares the rCBV for the whole region of interest with the histologic findings from the highest cellular-packing-attenuation region within that region of interest. Similarly, the maximum rCBV of the whole region of interest may be skewed by a single voxel with an abnormally high rCBV, as may occur with image noise[20] or in the vicinity of blood vessels.[21] Because these regions of interest were the site of biopsies, great care was taken to avoid including large vessels. Histogram analysis avoids the problem of single abnormal voxels.[20] Most interesting, our results suggest that it does not matter which method is used because all provided similar results.

One obvious limitation of this study is the small number of patients. We have, however, analyzed data from 38 biopsy sites in a fairly homogeneous group of patients (ie, similar grade and histologic type of tumor). We have deliberately avoided including data from patients with low-grade gliomas because their rCBV is also dependent on the histogenesis of the tumor, with oligodendrogliomas having higher rCBV values than astrocytomas.[22,23] Obviously the number of biopsies per patient has to be limited to avoid causing unnecessary morbidity.

We have also concentrated on a single measure of perfusion, namely rCBV. The reason for this is that this parameter is best characterized pathologically as a marker of tumor vascular attenuation/vascularity.[2,3] Other summary parameters (eg, time to peak, peak height, and percentage recovery) have not been so well characterized pathologically and, though commonly used, are also dependent on factors such as bolus volume and shape, injection rate, and cardiac output.[24]

In this study, we have deliberately not tried to correlate rCBV with tumor sections stained for vascular markers (eg, von Willebrand factor or CD34) because rCBV would be impossible to quantify in the small tissue samples because vessels would occupy <2% of the tumor tissue we obtained. Especially, therefore, we are unable to account for the location (gray, superficial white, deep white, deep gray) and orientation of the biopsy with respect to brain surface (right-angles, oblique, tangential) and the amount of native-versus-pathologic (endothelial-proliferative) vasculature.

Conclusions

The development of new agents for the treatment of brain tumors will require new methods of assessing response to therapy. Because it is clinically impossible to perform brain tumor biopsies at multiple time points due to the risk of complications, it is important that there are noninvasive methods that can probe tumor pathology. These methods can only be used if we understand what they show.

References

1. Brem S, Cotran R, Folkman J. **Tumor angiogenesis: a quantitative method for histologic grading.** *J Natl Cancer Inst* 1972;48:347–56
2. Aronen HJ, Gazit IE, Louis DN, et al. **Cerebral blood volume maps of gliomas: comparison with tumor grade and histologic findings.** *Radiology* 1994;191:41–51
3. Sugahara T, Korogi Y, Kochi M, et al. **Correlation of MR imaging-determined**

cerebral blood volume maps with histologic and angiographic determination of vascularity of gliomas. *AJR Am J Roentgenol* 1998;171:1479–86
4. Maia AC, Malheiros SM, da Rocha AJ, et al. **MR cerebral blood volume maps correlated with vascular endothelial growth factor expression and tumor grade in nonenhancing gliomas.** *AJNR Am J Neuroradiol* 2005;26:777–83
5. Sadeghi N, Salmon I, Decaestecker C, et al. **Stereotactic comparison among cerebral blood volume, methionine uptake, and histopathology in brain glioma.** *AJNR Am J Neuroradiol* 2007;28:455–61
6. Price SJ, Jena R, Burnet NG, et al. **Improved delineation of glioma margins and regions of infiltration with the use of diffusion tensor imaging: an image-guided biopsy study.** *AJNR Am J Neuroradiol* 2006;27:1969–74
7. Price SJ, Fryer TD, Cleij MC, et al. **Imaging regional variation of cellular proliferation in gliomas using 3′-deoxy-3′-[18F]fluorothymidine positron-emission tomography: an image-guided biopsy study.** *Clin Radiol* 2009;64:52–63. Epub 2008 Sep 4
8. Studholme C, Hill DL, Hawkes DJ. **Automated three-dimensional registration of magnetic resonance and positron emission tomography brain images by multiresolution optimization of voxel similarity measures.** *Med Phys* 1997;24:25–35
9. Ostergaard L, Sorensen AG, Kwong KK, et al. **High-resolution measurement of cerebral blood flow using intravascular tracer bolus passages. Part II. Experimental comparison and preliminary results.** *Magn Reson Med* 1996;36:726–36
10. Ostergaard L, Weisskoff RM, Chesler DA, et al. **High-resolution measurement of cerebral blood flow using intravascular tracer bolus passages. Part I. Mathematical approach and statistical analysis.** *Magn Reson Med* 1996;36:715–25
11. Smith AM, Grandin CB, Duprez T, et al. **Whole brain quantitative CBF and CBV measurements using MRI bolus tracking: comparison of methodologies.** *Magn Reson Med* 2000;43:559–64
12. Law M, Young R, Babb J, et al. **Histogram analysis versus region of interest analysis of dynamic susceptibility contrast perfusion MR imaging data in the grading of cerebral gliomas.** *AJNR Am J Neuroradiol* 2007;28:761–66
13. Gauvrit JY, Law M, Papadaki E, et al. **Dynamic susceptibility contrast perfusion MRI of angiogenesis and microscopic tumoral infiltration in the corpus callosum of patients with gliomas.** *Proc Intl Soc Mag Reson Med* 2006;14:822
14. Greene HS. **Heterologous transplantation of mammalian tumors.** *J Exp Med* 1941;73:461
15. Sadeghi N, D'Haene N, Decaestecker C, et al. **Apparent diffusion coefficient and cerebral blood volume in brain gliomas: relation to tumor cell density and tumor microvessel density based on stereotactic biopsies.** *AJNR Am J Neuroradiol* 2008;29:476–82
16. Noguchi T, Yoshiura T, Hiwatashi A, et al. **Perfusion imaging of brain tumors using arterial spin-labeling: correlation with histopathologic vascular density.** *AJNR Am J Neuroradiol* 2008;29:688–93
17. Henry RG, Vigneron DB, Fischbein NJ, et al. **Comparison of relative cerebral blood volume and proton spectroscopy in patients with treated gliomas.** *AJNR Am J Neuroradiol* 2000;21:357–66
18. Lehmann P, Vallee JN, Saliou G, et al. **Dynamic contrast-enhanced T2*-weighted MR imaging: a peritumoral brain oedema study.** *J Neuroradiol* 2009;36:88–92. Epub 2008 Dec 2
19. Tzika AA, Zarifi MK, Goumnerova L, et al. **Neuroimaging in pediatric brain tumors: Gd-DTPA-enhanced, hemodynamic, and diffusion MR imaging compared with MR spectroscopic imaging.** *AJNR Am J Neuroradiol* 2002;23:322–33
20. Emblem KE, Nedregaard B, Nome T, et al. **Glioma grading by using histogram analysis of blood volume heterogeneity from MR-derived cerebral blood volume maps.** *Radiology* 2008;247:808–17
21. Caseiras GB, Thornton JS, Yousry T, et al. **Inclusion or exclusion of intratumoral vessels in relative cerebral blood volume characterization in low-grade gliomas: does it make a difference?** *AJNR Am J Neuroradiol* 2008;29:1140–41
22. Lev MH, Ozsunar Y, Henson JW, et al. **Glial tumor grading and outcome prediction using dynamic spin-echo MR susceptibility mapping compared with conventional contrast-enhanced MR: confounding effect of elevated rCBV of oligodendrogliomas.** *AJNR Am J Neuroradiol* 2004;25:214–21
23. Cha S, Tihan T, Crawford F, et al. **Differentiation of low-grade oligodendrogliomas from low-grade astrocytomas by using quantitative blood-volume measurements derived from dynamic susceptibility contrast-enhanced MR imaging.** *AJNR Am J Neuroradiol* 2005;26:266–73
24. Calamante F, Thomas DL, Pell GS, et al. **Measuring cerebral blood flow using magnetic resonance imaging techniques.** *J Cereb Blood Flow Metab* 1999;19:701–35